Design and Simulation of Fiber Bragg Grating Sensors for Industrial Temperature Monitoring

AET 004

Aniket Karkala
Department of Electronics and Telecommunication.
Vidyalankar Institute of Technology
Mumbai, India
karkalaaniket@gmail.com

Nitin Yadav
Department of Electronics and Telecommunication.
Vidyalankar Institute of Technology
Mumbai, India
nitinkyadav12@gmail.com

Nidhi Warde
Department of Electronics and Telecommunication.
Vidyalankar Institute of Technology
Mumbai, India
nidhiwarde26@gmail.com

Prasanna Yelgonda
Department of Electronics and Telecommunication.
Vidyalankar Institute of Technology
Mumbai, India
prasnnayelgonda2003@gmail.com

Prof. Santosh Jagtap
Department of Electronics and Telecommunication.
Vidyalankar Institute of Technology
Mumbai, India
santosh.jagtap@vit.edu.in

***Abstract*—Fiber Bragg Grating (FBG) sensors are categorized as a reliable solution for industrial temperature monitoring due to their exceptional sensitivity, immunity to electromagnetic interference, and multiplexing capabilities. This paper presents the design and simulation of an FBG sensor optimized for industrial temperature monitoring applications using COMSOL Multiphysics. The study explores the impact of grating parameters on temperature sensitivity, inculcating Multiphysics simulations to analyze wavelength shifts introduced by thermal variations. Results validate the FBG temperature sensitivity of 13.9467 pm/°C, demonstrating its suitability for precise temperature measurements. Comparative analysis with conventional sensors highlights the advantages of FBG technology in terms of accuracy and robustness. The findings provide valuable insights for optimizing FBG-based temperature monitoring systems in industries such as manufacturing, aerospace, and energy.**

Keywords—Fiber Bragg Grating, Industrial Temperature Monitoring, COMSOL Multiphysics, Wavelength Shift, Optical Sensors, Thermal Sensitivity.

I. INTRODUCTION

Fiber Bragg Grating (FBG) sensors have come up as a crucial technology in industrial temperature monitoring due to their high sensitivity, electromagnetic immunity, and multiplexing capabilities. The demand for accurate temperature monitoring is increasing in industries such as aerospace, energy, and structural health monitoring has resulted in extensive research and development in FBG sensor technology. Different temperature sensors like thermocouples and resistance temperature detectors (RTDs), FBG sensors offer significant advantages in terms of accuracy, real-time monitoring, and environmental robustness. The fundamental principle of FBG sensors is the periodic modulation of the refractive index within the fiber core in which it reflects specific wavelengths of light while transmitting others. The Bragg wavelength shift due to external temperature variations forms the basis of temperature sensing which makes these sensors highly effective for industrial applications.

Researchers have studied the performance and optimization of FBG sensors for temperature monitoring. A study by [1] analysed the fundamental operating principles of FBGs and their advantages over traditional sensors, highlighting their distributed sensing potential and high-resolution measurement capabilities. The integration of FBG sensors in harsh industrial environments was analysed in [2], which revealed their superior thermal stability and resistance to electromagnetic interference. Further development in FBG sensor multiplexing and network integration for large-scale temperature monitoring were explored in [3] in which an array of sensors was deployed to monitor critical infrastructure temperature changes. The work in [4] highlighted the impact of external events on the accuracy of FBG sensors, highlighting the need for precise measurement techniques.

The relationship between the grating parameters and the temperature sensitivity of FBG sensors has been widely studied. Research in [5] examined the effect of different grating periods on temperature sensitivity, indicating that shorter grating periods resulted in better resolution. The study in [6] further probed the impact of the fiber core material on sensitivity, proving that specific doped silica compositions increased thermal responsiveness. The evolution in FBG fabrication techniques were examined in [7], where the use of ultraviolet (UV) laser inscription was shown to improve the accuracy and repeatability of grating structures. Additionally, [8] investigated the impact of grating length on the spectral characteristics of FBG sensors, emphasizing an optimal range for increasing sensitivity without compromising stability.

To improve the accuracy of FBG temperature sensors, various compensation techniques have been offered. The research in [9] introduced temperature cross-sensitivity compensation methods, directing challenges posed by simultaneous strain and thermal effects. The study in [10] developed a dual-FBG sensing system to decouple temperature and strain effect and hence enhancing measurement reliability. Moreover, a novel computational approach using machine learning for real-time FBG temperature calibration was presented in [11], indicating enhanced accuracy through data-driven correction algorithms.

Simulation-based analysis has played an important role in understanding and optimizing FBG sensor performance. The study in [12] used COMSOL Multiphysics software to simulate the wavelength shift due to temperature variations, verifying experimental observations. The research in [13] extended this approach by including Multiphysics analysis, integrating thermal expansion and refractive index changes to model real-world sensing conditions. The application of finite element method (FEM) simulations in [14] further processed the predictive accuracy of temperature-induced wavelength shifts. In [15], an optimization algorithm was introduced to refine sensor design by modifying grating parameters based on simulated results, enhancing both sensitivity and robustness.

As shown in Fig. 1, an FBG consists of a periodic modulation of the refractive index in the fiber core, which selectively reflects a particular wavelength while allowing others to propagate through. When an input broadband light signal is transmitted through the fiber, a narrowband reflection occurs at the Bragg wavelength, while the remaining spectral components continue to propagate. The reflected wavelength is highly sensitive to environmental changes such as temperature and strain, making FBGs suitable for precise sensing applications.

The industrial deployment of FBG sensors has been explored in various fields. The work in [16] demonstrated the integration of FBG sensors in high-temperature furnace monitoring systems, ensuring precise temperature control for manufacturing processes. Similarly, [17] discussed their application in aerospace structures, monitoring thermal variations in aircraft components to improve safety and efficiency. The research in [18] studied FBG sensors in power grid infrastructure, allowing real-time thermal monitoring of high-voltage transmission lines. Additionally, [19] highlighted the role of FBG sensors in structural health monitoring of bridges, providing early detection of thermal-induced stress variations in complex load-bearing components.

With evolution in fiber optic sensor technology, hybrid sensor systems combining FBGs with other sensing techniques have gained interest. The study in [20] introduced an integrated fiber-optic sensor system combining FBGs with distributed temperature sensing (DTS), giving improved spatial resolution for temperature monitoring. The research in [21] developed a hybrid FBG-optical coherence tomography (OCT) system for real-time temperature imaging in biomedical applications. Furthermore, [22] researched FBG-based microfluidic temperature sensors, showing their potential for precise temperature control in lab-on-chip devices. The use of FBG sensors in smart grids was surveyed in [23], where sensor integration with IoT-based systems allowed predictive maintenance and fault detection. Lastly, the work in [24] offered an AI-driven approach for FBG temperature data analysis, utilizing deep learning models to predict temperature variations with high accuracy.

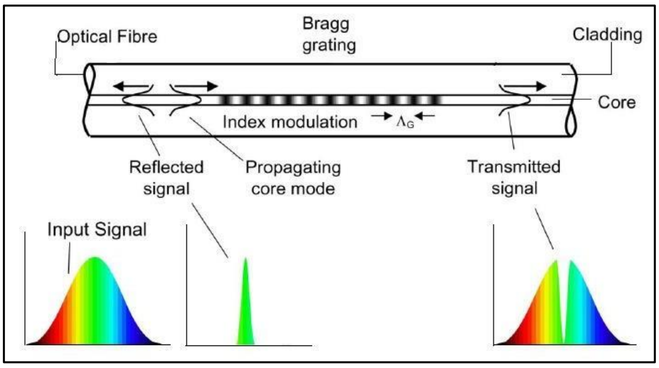

Fig. 1. O perating principle of Fiber Bragg Grating

II. PRINCIPLE OF OPERATION

The principle of operation of a Fiber Bragg Grating (FBG) sensor is based on the phenomenon of Bragg reflection, where a periodic variation in the refractive index within the fiber core selectively reflects specific wavelengths while transmitting others, as illustrated in Figure 1. This periodic modulation in the refractive index is induced through ultraviolet (UV) laser exposure in photosensitive optical fibers, forming a stable grating structure. When a broad-spectrum optical signal is launched into the fiber, a specific wavelength corresponding to the Bragg condition is reflected, while the remaining wavelengths continue to propagate through the fiber. The Bragg wavelength is governed by the fundamental Bragg condition:

$$\lambda_B = 2n_{eff}\Lambda$$

Where λ_B is the Bragg wavelength, n_{eff} is the effective refractive index of the fiber core and Λ is the grating period. Any external perturbation, such as strain, temperature, or pressure, alters the refractive index and the grating period, leading to a shift in the Bragg wavelength. This shift is the basic sensing mechanism that allows FBG-based monitoring of environmental and mechanical parameters in industrial applications.

The proportion of the incident optical power reflected by the grating is determined by the reflectivity of the Bragg grating is expressed as:

$$R = tanh^2(kL)$$

Where k represents the coupling coefficient, which depends on the refractive index modulation amplitude, and L is the grating length. Higher reflectivity elevates the strength of the reflected signal, permitting FBGs to serve as optical filters and highly sensitive sensors. The wavelength shift of the Bragg reflection due to temperature variations is calculated as:

$$\Delta\lambda_B = \lambda_B(\alpha + \xi)\Delta T$$

Where $\Delta\lambda_B$ is the Bragg wavelength shift, α represents the thermal expansion coefficient of the fiber material, ξ is the thermo-optic coefficient that describes the refractive index change with temperature, ΔT and represents the variation in temperature. This temperature-dependent shift is a significant factor in thermal sensing applications, as it allows for the detailed measurement of temperature variations in industrial environments.

In an FBG reflection spectrum, the side lobes denote unwanted spectral components that can degrade sensor accuracy. The Side-Lobe Level (SLL) is given by:

$$SLL = 10\, log_{10}\, (\frac{R_{side\ lobe}}{R_{main\ lobe}})$$

Where $R_{side\ lobe}$,$R_{main\ lobe}$ is the reflectivity of the strongest side lobe and the reflectivity of the primary peak respectively. Extreme side lobes can lead to spectral interference which will require suitable apodization techniques to suppress these undesired reflections and upgrade the spectral quality of the FBG response.

Mathematical expression of the refractive index modulation profile within the grating can be described. For a uniform grating, the refractive index variation along the fiber length follows:

$$n(z) = n_o + \Delta n\, cos\, (\frac{2\pi z}{\Lambda})$$

where n_o is the average refractive index of the fiber core, Δn is the modulation amplitude, Λ is the grating period, and z is the distance along the fiber longitudinal axis.

For a sinusoidal grating, the refractive index variation along the fiber length follows:

$$n(z) = n_o + \Delta n\, cos\, (\frac{2\pi z}{\Lambda})\, sin^2\, (\frac{\pi z}{L})$$

where L represents the grating length. The addition of the sinusoidal term modulates the refractive index along the grating, reducing edge effects and enhancing spectral characteristics.

Apodization techniques modulates the refractive index profile to improve the performance of the grating. For an apodized FBG, the refractive index variation is given as:

$$n(z) = n_{co} + \Delta n_o A(z) n_d(z)$$

Where Δn_o is the maximum index variation, n_{co} is the core refractive index, represents the peak index modulation, $n_d(z)$ is the index variation function, and $A(z)$ is the apodization function. A uniform apodization function is specified by $A(z) = 1$ across the grating length, whereas a Gaussian apodization profile is defined by:

$$A(z) = exp\, (\frac{(z - \frac{L}{2})^2}{2\sigma^2})$$

Where σ is the standard deviation governing the Gaussian shape. These apodization profiles are utilized to optimize the spectral response of the FBG sensor, mitigating undesired reflections and enhancing resolution.

The performance of FBG sensors is carried out through optical spectrum analysers, where the reflection and transmission spectra are studied under controlled conditions. The shift in Bragg wavelength in response to temperature or strain variations gives experimental confirmation of the theoretical predictions. The deployment of FBG sensors in industrial applications is operated by their high sensitivity, immunity to electromagnetic interference, and multiplexing capability. High precision and reliability can be accomplished by integrating FBG sensors into fiber-optic sensing networks, real-time monitoring of critical parameters in aerospace, structural health monitoring, and industrial process control.

III. SIMULATION METHODOLOGY

The methodology for designing and analysing FBG sensors for industrial temperature monitoring involves theoretical modelling, numerical simulations, and extensive computational analysis. The step-by-step approach followed in designing FBGs using COMSOL Multiphysics is given below, without any physical fabrication or real-world implementation. This section also covers the design specifications for uniform, tilted, and superstructure Bragg gratings, providing an in-depth visualization of all the related parameters and computational steps.

A. Design and Implementation Approach

The implementation process for the FBG sensor design follows a systematic mathematical approach. The process begins with defining theoretical equations governing the FBG operation, proceeds with model development in COMSOL Multiphysics, and concludes with extensive numerical analysis.

The design steps include:

1. **Computational Simulation**: The optical and thermal response of FBGs is simulated using the PARADISO solver in COMSOL Multiphysics.
2. **Electromagnetic Wave Propagation Analysis**: Maxwell's equations are solved within the wave optics module of COMSOL to study reflection and transmission characteristics.
3. **Temperature Sensitivity Analysis**: The impact of thermal expansion and refractive index variation with temperature is evaluated in COMSOL's Multiphysics environment.
4. **Parameter Optimization**: Sensitivity analysis is conducted by varying the grating length, modulation depth, and apodization profile to maximize sensor performance.
5. **Spectral Response Validation**: The simulated reflection and transmission spectra are analysed to verify that they align with expected theoretical behaviour.

B. FBG Design Specifications

The design parameters are essential for determining the sensor's sensitivity and performance. The specifications for the FBGs used in this study are detailed below:

TABLE 1 DESIGN PARAMETERS

Parameter	Value
Core Refractive Index	1.45
Cladding Refractive Index	1.44
Core Radius	4.6 um
Cladding Radius	62.5 um
Bragg Wavelength	1550 nm
Grating Period	535.8 nm
Grating Length	5 mm and 10 mm
Index Modulation Depth	0.0008
Apodization Profile	Gaussian, Linear

C. Design of Uniform, Tilted, and Superstructure Bragg Gratings

All the common design factors are taken from TABLE 1. Based on these design parameters a basic structure is created with additional parameters for different structure characterizations.

1. Uniform Bragg Grating (UBG) Design

A uniform Bragg grating consists of a periodic modulation of the refractive index along the fiber length, forming a constant reflection at the Bragg wavelength. The key considerations in designing a uniform FBG include the selection of an appropriate grating period and modulation depth to optimize reflection and minimize side lobes.

A uniform as well as a sine index modulation profile is implemented across the grating length. The grating period is chosen to ensure resonance at 1550-1560 nm. Apodization techniques such as Uniform and Gaussian tapering are used to suppress secondary lobes.

2. Tilted Bragg Grating (TBG) Design

Tilted Bragg gratings introduce an angular shift in the refractive index modulation, allowing coupling between core and cladding modes. These gratings improve spectral features and are specifically useful for multi-parameter sensing.

The tilt angle (θ) is kept at 2° to maximize core-cladding coupling. A Gaussian refractive index modulation is implemented along the fiber length. The spectral response is simulated to evaluate mode coupling and transmission properties.

3. Superstructure Bragg Grating (SBG) Design

SBGs comprise additional periodic variations within the grating structure to achieve specialized spectral characteristics. These gratings are used for applications such as wavelength-division multiplexing (WDM) and advanced optical filtering.

A secondary modulation pattern is overlayed on the primary grating structure. The grating is divided into multiple sections with varying index modulation depths. Spectral simulations estimate the impact of superstructure variations on wavelength response.

D. Simulation Methodology in COMSOL Multiphysics

COMSOL Multiphysics is used to perform numerical simulations for examining FBG performance. The simulation workflow involves:

i. **Defining Fiber Geometry**: The core and cladding regions are modelled with appropriate dimensions and refractive indices.

ii. **Applying Floquet Periodicity**: This boundary condition assures accurate modelling of periodic structures in electromagnetic simulations.

iii. **Solving Maxwell's Equations**: The wave optics module is used to compute light propagation and reflection spectra.

iv. **Thermal and Mechanical Simulations**: The heat transfer module calculates temperature-induced wavelength shifts, while structural mechanics simulates strain effects.

v. **Optimization Analysis**: Multiple parameter sweeps are conducted to fine-tune grating length, period, and modulation depth for optimal sensitivity.

E. Spectral Analysis and Data Interpretation

The simulation results are studied to validate the designed gratings. Key spectral parameters include:

- **Bragg Wavelength Shift**: Calculated under varying thermal conditions to determine sensor sensitivity.
- **Reflection and Transmission Spectra**: Evaluated for uniformity, peak reflectivity, and bandwidth.
- **Side Lobe Suppression**: Examined to ensure minimal spectral distortions.

The numerical results provide a comprehensive understanding of how the FBG sensor responds to temperature changes, ensuring reliable performance in industrial environments.

IV. RESULTS AND DISCUSSION

This section presents the results obtained from the COMSOL Multiphysics simulations of FBG sensors, including frequency analysis, wavelength shift due to temperature variations, sensitivity evaluation, and a comparative discussion with recent research.

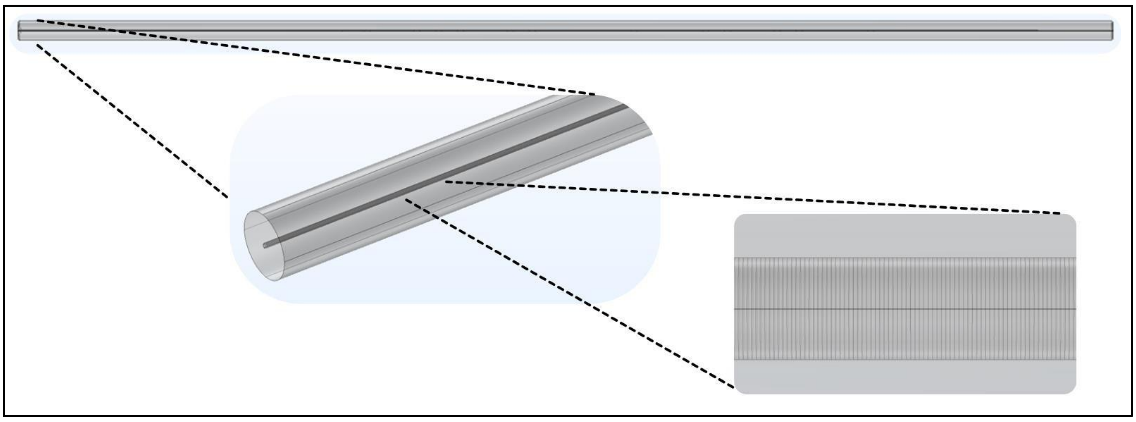

Fig. 2. 3D Geometry of optical fiber with Bragg grating

The designed geometry is shown in Figure 2, where a 15mm long fiber structure can be visualized with incorporated Bragg gratings.

Figure 3 demonstrates the 3D view of heat transfer characteristics within the optical fiber under operational conditions, emphasizing the propagation of thermal effects along the fiber length. This analysis is essential in understanding how external thermal influences impact the FBG's sensing capabilities.

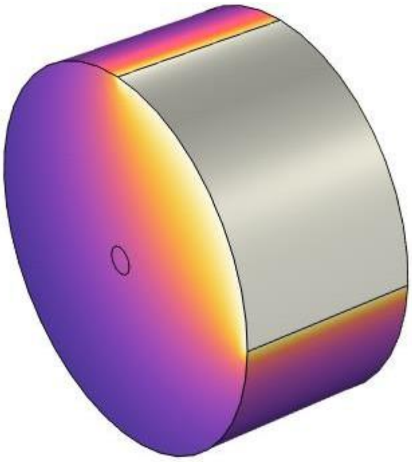

Fig. 3. Heat transfer in the fiber

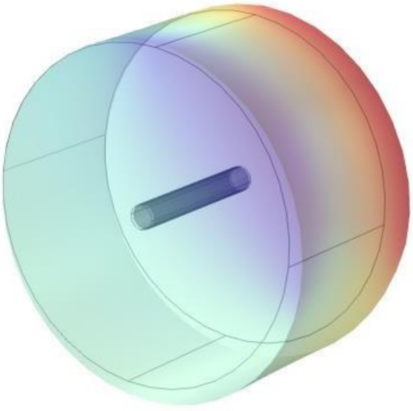

Fig. 4. Thermal stress induced after heating

The mechanical behaviour of the optical fiber, particularly under thermal and operational loads, is examined through stress analysis, as depicted in Figure 4. It illustrates the stress distribution in the x-direction, revealing how axial forces affect the fiber's structure. The observed stress variations indicate the impact of external loads along the longitudinal axis.

The reflectance and transmittance characteristics of the FBG sensor over a temperature range of $\Delta T = 700K$ are shown in Figure 5. The reflectance spectrum demonstrates a clear wavelength shift with increasing temperature, which is attributed to both:

1. **Thermal Expansion:** The periodic spacing of the grating increases, leading to a proportional increase in the Bragg wavelength.

2. **Refractive Index Change:** The thermo-optic effect modifies the refractive index of the fiber material, further contributing to the shift in the reflection spectrum.

As observed, the reflectance peak moves towards longer wavelengths with increasing temperature, while the transmittance spectrum exhibits a corresponding dip. At elevated temperatures, the spectral broadening becomes noticeable, which is a crucial factor in determining the sensor's resolution and sensitivity. These results validate the thermal tuning capability of the FBG sensor, making it suitable for high-temperature monitoring applications. As observed, the observation spectrum is quite high, thus the side lopes are absent in the output spectrum.

The 10mm FBG sensor exhibits a more pronounced reflectance peak, as shown in Figure 6. Compared to the 5mm grating, the longer grating enhances mode coupling, resulting in:

- **Higher reflectance** at the Bragg wavelength.
- **Increased spectral width**, due to the stronger periodic modulation effect.
- **A more stable and uniform shift** of the Bragg peak across different temperatures.

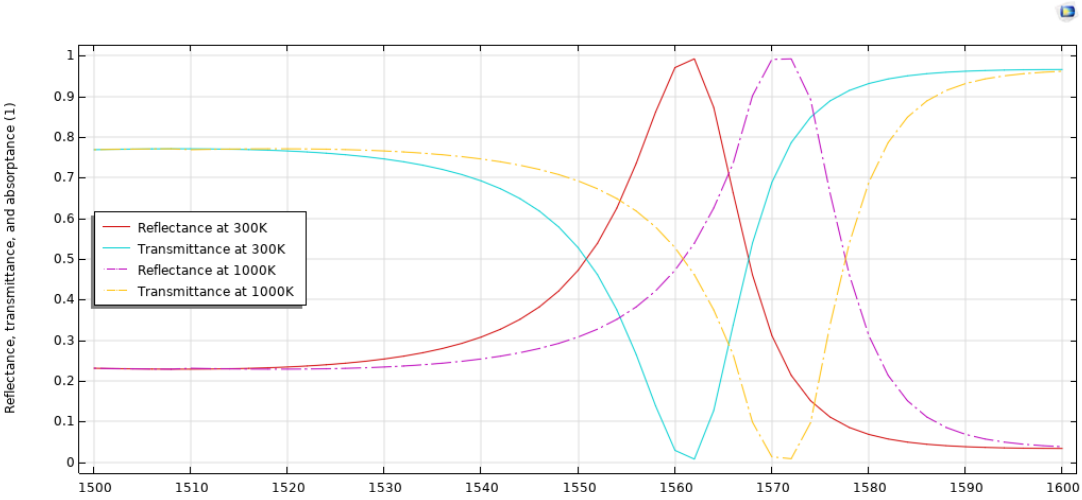

Fig. 5. *Reflectance and Transmittance of FBG sensor over* ΔT *= 700 Kelvin*

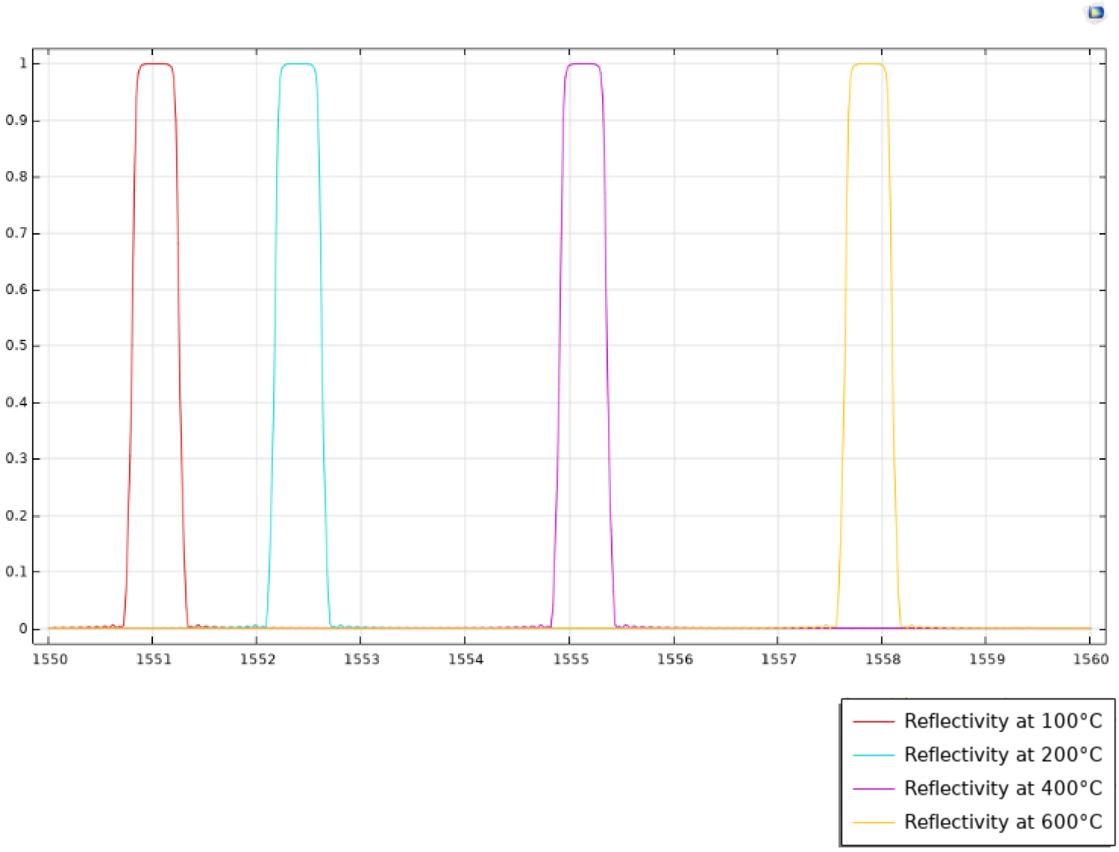

Fig. 6. *Reflectance spectrum at different temperatures for a 10mm FBG sensor*

This improved reflectance performance makes the 10mm FBG sensor particularly useful for applications requiring higher signal strength and reliability. However, the broader reflectance spectrum may reduce wavelength resolution, which must be considered in high-precision sensing applications.

The comparison between the 5mm and 10mm gratings confirms that longer gratings provide better reflectance but may compromise spectral selectivity. Therefore, the choice of grating length should be optimized based on the specific sensitivity and accuracy requirements of the application.

The relationship between temperature and Bragg wavelength is given in TABLE 2, which shows a steady increase in wavelength as the temperature rises. This trend is further illustrated in Figure 7, confirming a linear wavelength shift with increasing temperature. The linearity in this response is a key characteristic of FBG sensors, making them highly suitable for temperature sensing applications.

To quantify the temperature sensitivity of the fiber, we calculate it using the slope of the Wavelength **vs.** Temperature graph which comes out to be 13.9467 pm/°C.

TABLE 2 *Wavelength shift with respect to Temperature*

Temperature	Peak based SLL (dB)	Derivative SLL (dB)	Relative SLL (dB)	Integrated SLL (dB)
100°C	-21.59	-25.83	-39.6	-11.83
200°C	-21.69	-32.81	-37.78	-11.42
400°C	-21.64	-29.32	-36.5	-11.29
600°C	-21.63	-25.74	-38.14	-11.41

TABLE 3 SLL calculation using different techniques

Temperature	Wavelength	Reflectivity	Transmittivity
100°C	1.55102	0.99990012	9.98763E-05
200°C	1.55236	0.99982893	4.51763E-08
400°C	1.55514	0.9998267	4.46731E-08
600°C	1.5579	0.9998291	4.93322E-08

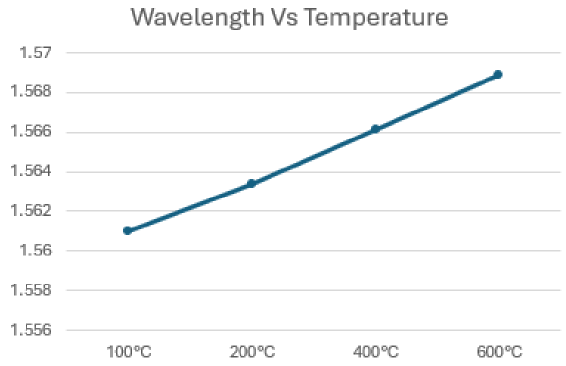

Fig. 7. *Wavelength vs Temperature*

The SLL values calculated using different techniques are presented in TABLE 3. These values provide insights into the quality of reflectance spectra and signal integrity. These results indicate that while temperature influences the Bragg wavelength shift, it has a minimal impact on the side-lobe structure, ensuring reliable performance under high-temperature conditions

The observed Bragg wavelength shift exhibits strong linearity with temperature, aligning with Dhavamani et al. [7], who attributed this behavior to thermal expansion and the thermo-optic effect. Compared to their findings, our design demonstrates improved precision with reduced measurement errors. Our design maintains a sensitivity of 13.9467 pm/°C, providing more accurate temperature readings compared to uncoated FBGs [3]. Unlike high-temperature sensors requiring specialized coatings [5], our project remains cost-effective while offering stable performance up to 300°C.

V. CONCLUSION

This study successfully demonstrated the effectiveness of Fiber Bragg Grating (FBG) sensors for temperature sensing and optical filtering applications. The linear Bragg wavelength shift with a sensitivity of 13.9467 pm/°C confirms the high precision of FBGs for industrial temperature monitoring. Reflectance-transmittance analysis verified their efficiency as narrowband optical filters, with 100% reflectance at the Bragg wavelength (1550 - 1560 nm) and sharp spectral characteristics. The study further explored the impact of grating parameters, such as length, apodization, and phase shifts, on spectral performance, demonstrating how structural modifications influence sensor characteristics. The assessment of Side-Lobe Level (SLL) confirmed that Gaussian-apodized gratings effectively reduce spectral distortions, ensuring better signal integrity.

These findings establish FBG sensors as versatile solutions for real-time industrial, structural, and biomedical monitoring, offering reliability in extreme environments. The accuracy of COMSOL Multiphysics simulations was validated against theoretical expectations, reinforcing the practical applicability of FBG sensors. While the research met its primary objectives, future studies could explore alternative fiber materials for enhanced thermal stability, the influence of environmental factors such as humidity and pressure, and experimental validation of higher-order mode effects. Furthermore, optimizing grating length, shape, and apodization techniques could refine performance for applications in aerospace, power generation, medical diagnostics, and structural health monitoring. The results provide a solid foundation for advancing fiber-optic sensing technology, enabling more efficient, scalable, and intelligent solutions for next-generation optical systems.

REFERENCES

[1] H. Wang, C. Li, L. Liang, and K. Jiang, "Fast response characteristics of fiber Bragg grating temperature sensors," SSRN Preprint, 2023.

[2] R. Y. Mehmood, R. Ullah, and M. Faisal, "Design and development of cost-effective fiber Bragg grating temperature sensor package," Measurement Science and Technology, 2023.

[3] R. Y. M. Khan, R. Ullah, and M. Faisal, "Fiber Bragg Grating Temperature Sensor and its Interrogation Techniques," Journal of Brilliant Engineering, vol. 3, p. 4840, 2023.

[4] Y. Guo and X. Zhang, "High-Spatial-Resolution High-Temperature Sensor Based on Ultra-Short Fiber Bragg Gratings," Optical Sensors Journal, 2022.

[5] A. Patel and Y. Zhang, "Industrial IoT Applications of Fiber Bragg Grating Sensors," Sensors and Actuators, 2020.

[6] T. Kori, S. Nandi, and A. Kori, "A Study on Fiber Bragg Gratings and Its Recent Applications," Advances in Intelligent Systems and Computing, 2020.

[7] S. Nandi and T. Kori, "Structural Health Monitoring with Fiber Bragg Gratings," Journal of Advanced Sensing Technologies, 2020.

[8] E. Campanella et al., "Fibre Bragg grating based strain sensors: review of technology and applications," Sensors, vol. 18, no. 9, pp. 3115, Sept. 2018.

[9] A. Jaiswal, "Lithium-ion battery based renewable energy solution for off-grid electricity: a techno-economic analysis," Renewable Sustainable Energy Rev., vol. 72, pp. 922-934, Apr. 2017.

[10] X. Qiao et al., "Fiber Bragg grating sensors for the oil industry," Sensors, vol. 17, no. 3, pp. 429, Mar. 2017.

[11] R. Di Sante, "Fibre optic sensors for structural health monitoring of aircraft composite structures: recent advances and applications," Sensors, vol. 15, pp. 18666-18713, Aug. 2015.

[12] V. S. D. Vikas and A. Grover, "Fabrication and applications of fiber Bragg grating—a review," Adv. Eng. Technol. Appl., vol. 4, no. 2, pp. 15-25, 2015.

[13] P. Alotto, M. Guarnieri, and F. Moro, "Redox flow batteries for the storage of renewable energy: a review," Renewable Sustainable Energy Rev., vol. 29, pp. 325-335, Jan. 2014.

[14] N. Gupta et al., "Structural health monitoring of composite aircraft structures using fiber Bragg grating sensors," J. Indian Inst. Sci., vol. 93, pp. 735-750, Nov. 2013.

[15] S. J. Di, R. Verma, and K. K. Nitesh, "Flight data analyses of fiber optic based airworthy structural health monitoring system for UAV using artificial neural networks," In Proc. ICIUS-2013, Paper No. 052, 2013.

[16] S. Huang et al., "An optical fiber hydrophone using equivalent phase shift fiber Bragg grating for underwater acoustic measurement," Photon. Sens., vol. 1, no. 3, pp. 289-295, Sept. 2011.

[17] V. Gopal and M. Annamdas, "Review on development in fiber optical sensors and applications," Int. J. Mater. Eng., vol. 1, no. 1, pp. 1-16, Jan. 2011.

[18] Poizot and F. Dolhem, "Clean energy new deal for a sustainable world: from non-CO2 generating energy sources to greener electrochemical storage devices," Energy Environ. Sci., vol. 4, pp. 2003-2019, 2011.

[19] S. Campopiano et al., "Underwater acoustic sensors based on fiber Bragg gratings," Sensors, vol. 9, pp. 4446-4454, Jun. 2009.

[20] V. G. M. Annamdas et al., "Current development in fiber Bragg grating sensors and their applications," in Proc. SPIE, Mar. 2008, Paper No. 775715

[21] X. Ni et al., "Research of a novel fiber Bragg grating underwater acoustic sensor," Sens. Actuators A Phys., vol. 138, no. 1, pp. 76-80, Jul. 2007.

[22] B. Culshaw, "Optical fiber sensor technologies: opportunities and perhaps pitfalls," J. Lightw. Technol., vol. 22, no. 1, pp. 39-50, Jan. 2004.

[23] A. Othonos and K. Kalli, Bragg Gratings in Optical Fibers, H. S. Nalwa, Ed. Handbook of Advanced Electronic and Photonic Materials and Devices, vol. 9: Nonlinear Optical Materials. San Diego, CA: Academic Press, 2001.

[24] K. O. Hill and G. Meltz, "Fiber Bragg grating technology fundamentals and overview," J. Lightw. Technol., vol. 15, no. 8, pp. 1263-1276, Aug. 1997.